IOPscience iopscience.iop.org

Home Search Collections Journals About Contact us My IOPscience

A comparative study of the magnetization process of two-dimensional antiferromagnets

This article has been downloaded from IOPscience. Please scroll down to see the full text article.

1999 J. Phys.: Condens. Matter 11 4697

(http://iopscience.iop.org/0953-8984/11/24/311)

View the table of contents for this issue, or go to the journal homepage for more

Download details:
IP Address: 171.66.16.214
The article was downloaded on 15/05/2010 at 11:50

Please note that terms and conditions apply.

J. Phys.: Condens. Matter **11** (1999) 4697–4713. Printed in the UK PII: S0953-8984(99)01955-4

A comparative study of the magnetization process of two-dimensional antiferromagnets

A Honecker

Institut für Theoretische Physik, ETH-Hönggerberg, CH-8093 Zürich, Switzerland

E-mail: honecker@itp.ethz.ch

Received 19 February 1999, in final form 21 April 1999

Abstract. Plateaux in the magnetization curves of the square-, triangular- and hexagonal-lattice spin-1/2 XXZ antiferromagnet are investigated. One finds a zero-magnetization plateau (corresponding to a spin gap) on the square and hexagonal lattice with Ising-like anisotropies, and a plateau with one-third of the saturation magnetization on the triangular lattice which survives a small amount of easy-plane anisotropy. Here we start with transfer-matrix computations for the Ising limit and continue with series in the XXZ anisotropy for plateau boundaries using the ground states of the Ising limit. The main focus is then a numerical computation of the magnetization curves with anisotropies in the vicinity of the isotropic situation. Finally, we discuss the universality class associated with the asymptotic behaviour of the magnetization curve close to saturation, as observed numerically in two and higher dimensions.

1. Introduction

The discovery of high-T_c superconductivity has revived interest in two-dimensional Heisenberg antiferromagnets (for a review see [1]), since the CuO_2 planes give rise to a good realization of the $S = 1/2$ square-lattice antiferromagnet. Due to the large coupling constants of the high-T_c materials, the main focus is on properties in zero or small external magnetic fields. Nevertheless, it has also been progressively realized that antiferromagnets exhibit interesting phenomena in strong external magnetic fields, namely plateaux in their magnetization curves at certain fractions of the saturation value of the magnetization.

In one dimension, the appearance of plateaux in magnetization curves is by now rather well understood in terms of a quantization condition on the magnetization that involves the volume of a translationally invariant unit cell [2–8]. In fact, if the interaction inside finite clusters of spins is large with respect to the other interactions, the appearance of plateaux is governed by the volume of such a cluster irrespective of the dimension [8]. However, the simplest two-dimensional systems have equal coupling constants, and then it is less clear what determines the appearance of plateaux in magnetization curves. One well-known example of such plateaux in two dimensions is a plateau at one-third of the saturation magnetization in the triangular-lattice antiferromagnet. There have in fact been a number of theoretical studies of the magnetization process of two-dimensional triangular antiferromagnets (see [9–15] for a selection) which are at least to some extent motivated by the presence of this plateau or the more general feature of frustration. The number of recent investigations of the magnetization process of the square-lattice antiferromagnet [16–20] still seems to be smaller, and for the

0953-8984/99/244697+17$19.50 © 1999 IOP Publishing Ltd

hexagonal lattice we are aware of just a single study of the Ising antiferromagnet in a magnetic field [21].

The magnetization plateau of the triangular-lattice antiferromagnet can be observed experimentally in a variety of materials (see e.g. [22] for recent rather clear examples and [23] for a review of experimental facts about triangular-lattice antiferromagnets). The present investigation was in fact originally motivated by a magnetization experiment on the stacked triangular-lattice antiferromagnet $CsCuCl_3$ [24] which shows a plateau in the magnetization curve at one-third of the saturation value if the field is applied perpendicular to the c-axis. In many cases and in particular in $CsCuCl_3$, the spin is carried by a Cu^{2+} ion, giving rise to a spin $S = 1/2$. Furthermore, at least in $CsCuCl_3$, anisotropy of the interaction is important. This led us to considering a spin-$1/2$ XXZ model and to investigating the effect of the XXZ anisotropy Δ. The relevance of the results of the present paper for $CsCuCl_3$ will be discussed elsewhere [25].

The focus of the present work are general features, namely in which situations magnetization plateaux arise in two dimensions and the universality class of the transition to saturation. These questions will be investigated by computing the zero-temperature magnetization process of the $S = 1/2$ XXZ model on the aforementioned three lattice types, i.e. on a square, triangular and hexagonal lattice. This problem is described by the following Hamiltonian:

$$H = J \sum_{\langle \vec{x}, \vec{y} \rangle} \{ \Delta S^z_{\vec{x}} S^z_{\vec{y}} + \tfrac{1}{2} (S^+_{\vec{x}} S^-_{\vec{y}} + S^-_{\vec{x}} S^+_{\vec{y}}) \} - h \sum_{\vec{x}} S^z_{\vec{x}} \tag{1.1}$$

where the $\vec{S}_{\vec{x}}$ are spin-$1/2$ operators acting at $\vec{x}$ and h is a dimensionless magnetic field. The notation $\langle \vec{x}, \vec{y} \rangle$ denotes neighbouring pairs on a lattice whose total number of sites we denote by V. The magnetization $\langle M \rangle$ is given by the expectation value of the operator $M = (2/V) \sum_{\vec{x}} S^z_{\vec{x}}$ where the prefactor is chosen in order to normalize the saturation value to $\langle M \rangle = \pm 1$. The magnetization operator M commutes with the Hamiltonian (1.1). This leads to a technically useful simplification since it allows one to relate all properties in a magnetic field h to those at $h = 0$ with a suitably fixed magnetization $\langle M \rangle$.

The plan of this paper is as follows. First, we compute magnetization curves for the Ising model which is obtained from (1.1) by dropping the S^+S^- hopping-matrix elements. Exact zero-temperature ground states are readily written down for all plateaux observed in this limit. We then use this as an input to compute perturbation series in Δ^{-1} for the gap of single-spin excitations above these ground states. Even though the boundaries of plateaux are in general determined by multi-spin excitations, the series for the single-spin excitations yield a guide in which region the plateaux persist for $\Delta < \infty$. In addition to such a disappearance of plateaux existing in the Ising limit, further plateaux might open in other regions of Δ. This and the intrinsic limitations of a perturbative approach necessitate a direct computation of the magnetization process of the full quantum Hamiltonian (1.1), in particular in the region where Δ is of order unity. The bulk of the paper is therefore devoted to a numerical investigation of (1.1) on all three lattice types which is much in the spirit of classical work on single Heisenberg chains [26, 27]. Finally, we discuss the universality class associated with the asymptotic behaviour of the magnetization curve close to saturation, i.e. for $\langle M \rangle \to 1$.

2. The Ising antiferromagnet

The simplest case where one can observe magnetization plateaux in two dimensions is that of the Ising antiferromagnet. The latter can be obtained from (1.1) by taking the limit $\Delta \to \infty$

and rescaling $J \to J/\Delta$. This yields the energy function

$$E(\{s_{\vec{x}}\}) = \frac{J}{4} \sum_{\langle \vec{x},\vec{y} \rangle} s_{\vec{x}} s_{\vec{y}} - \frac{h}{2} \sum_{\vec{x}} s_{\vec{x}} \tag{2.1}$$

where the $s_{\vec{x}}$ are now Ising variables with $s_{\vec{x}} = \pm 1$. Note that here we use unusual conventions for J and h in order to simplify making contact with the XXZ Hamiltonian later.

While in the bulk of the paper we restrict consideration to zero temperature, here it is actually useful to work at finite inverse temperature β in order to permit application of the transfer-matrix method (see e.g. [28]). The magnetization is then given by

$$\langle M \rangle = \left(\sum_{\{s_{\vec{x}}\}} s_{\vec{y}} \mathrm{e}^{-\beta E(\{s_{\vec{x}}\})} \right) \Big/ \left(\sum_{\{s_{\vec{x}}\}} \mathrm{e}^{-\beta E(\{s_{\vec{x}}\})} \right). \tag{2.2}$$

Note that due to thermal fluctuations, M is no longer a conserved quantity and therefore one cannot drop the expectation values. Working with expectation values would also be mandatory for an anisotropy axis which does not coincide with the field direction, but this is not considered in the present paper.

In principle, one could directly write down zero-temperature ground states of (2.1) and compute the values of h where one of them becomes preferred to others. Actually, a complete set of ground states is known since the two-dimensional Ising model in the presence of an external magnetic field was already studied some time ago on the square lattice (see e.g. [29]), the triangular lattice (see e.g. [30]) and somewhat more recently on the hexagonal lattice [21].

However, since we later wish to build on the results for this limit, we believe that it is still useful to summarize the results in a uniform framework. We therefore evaluate (2.2) on a strip using the transfer-matrix method [28], where we employ periodic boundary conditions along the short direction of the strip and open ones in the long one. The site $\vec{y}$ in (2.2) is put at the centre of the strip.

Figure 1 shows magnetization curves obtained in this manner on a square, triangular and hexagonal lattice. The strip for figure 1 was in each case chosen to be 1000 sites long and 18 sites wide. A computation with the same length but half the width (i.e. ten sites for the square and hexagonal lattice, but nine for the triangular one) leads to values for $\langle M \rangle$ which are extremely close to the ones shown. In fact, the differences are numerically undetectable except

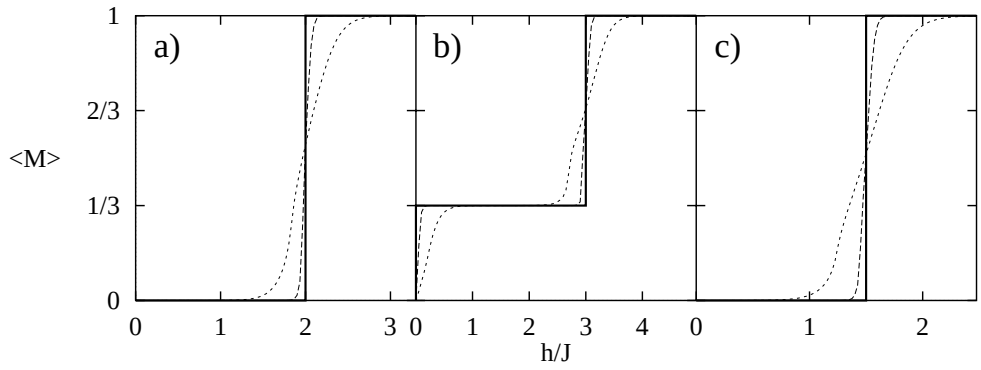

Figure 1. Magnetization curves of an Ising antiferromagnet on a 18×1000 (a) square, (b) triangular and (c) hexagonal lattice. The curves are for $J\beta = \infty$ (full), $J\beta = 40$ (long dashes) and $J\beta = 8$ (short dashes).

in the vicinity of the zero-temperature critical fields†, but the difference with respect to the results shown in figure 1 never exceeds 10^{-2}. We may therefore expect that the magnetization curves in figure 1 are basically indistinguishable from those of the thermodynamic limit. The smallness of finite-size effects will be a justification for using small system sizes later in the analysis of the XXZ antiferromagnet, although then finite-size corrections should be considered.

The interpretation of figure 1 is as follows. Both the square and hexagonal lattices are bipartite lattices. Thus, their zero-temperature ground state at sufficiently small fields is given by all spins pointing up on one sublattice and pointing down on the other. If the magnetic field becomes large enough to make it favourable to align one further spin along the field, it becomes so for all, and one has a sharp transition from the unmagnetized antiferromagnetic ground state to a fully magnetized ferromagnetic one. The transition field is readily found by computation to equal $h = 2J$ or $h = \frac{3}{2}J$ for the square and hexagonal lattice, respectively (in fact, it is easy to see that the transition to a fully magnetized state takes place at $h = (z/2)J$, where z is the coordination number of the lattice).

The situation is slightly different for the triangular lattice where each plaquette is frustrated. This lattice has three sublattices and energy is minimized at small fields by aligning all spins in two of them along the field and the ones in the third in the opposite direction. Increasing the field, it again becomes favourable for all of the latter spins simultaneously to align also along the field. Thus one obtains a sharp first-order transition from a state with $\langle M \rangle = 1/3$ to the fully magnetized one at $h = 3J$.

At non-zero temperature ($\beta < \infty$), the corners of the magnetization plateaux are smoothed out by thermal fluctuations and one sees no sharp transitions in the magnetization curve. This simply means that $\langle M \rangle$ is not a good quantity for detecting the thermodynamic phase transitions which at finite temperature should replace the boundaries of the zero-temperature magnetization plateaux. Since the smoothing effect of thermal fluctuations is actually not desired when one studies magnetization plateaux, we will restrict consideration from now on to zero temperature. It should, however, be noted that non-zero temperature would have effects on the XXZ model that are qualitatively similar to those discussed above for the Ising model.

3. Expansions around the Ising limit

Following this illustrative study of the Ising antiferromagnet, we now turn to the XXZ model (1.1). We use the ground states described in the previous section to expand the gap of single-spin excitations in powers of Δ^{-1}.

Since we wish to cover a variety of cases, it is convenient to use a simple but general method for higher-order series expansions of a quantum mechanical system which is summarized e.g. in section 3 of [31]. This should be sufficient to obtain an overview, but could certainly be extended to higher orders using more sophisticated cluster expansions if this should turn out to be desirable for concrete applications.

For the *square* and *hexagonal* lattice there is just a plateau at $\langle M \rangle = 0$. The lowest excitations are those where a single spin is flipped with respect to the antiferromagnetic ground state. Due to the antiferromagnetic nature of the ground state, the first-order corrections to the energies vanish and one finds a non-trivial dispersion only in second order in Δ^{-1}. Since both cases have been studied in detail in [32] (see also references therein) and [33], respectively, we skip the details of the computation.

† A clear phase transition should be observable in thermodynamic quantities at the location of these maxima of the finite-size effects.

Analytical fourth-order expressions for the gap of these excitations with $S^z = 1$ are given by

$$m = J\left(2\Delta - \frac{5}{3\Delta} + \frac{137}{432\Delta^3}\right) + \mathcal{O}(\Delta^{-4}) \tag{3.1}$$

for the *square* lattice, and

$$m = J\left(\frac{3}{2}\Delta - \frac{15}{8\Delta} + \frac{295}{128\Delta^3}\right) + \mathcal{O}(\Delta^{-4}) \tag{3.2}$$

for the *hexagonal* lattice. Numerical versions of the coefficients up to tenth order can be found in table I of [32] and [33], respectively. Applying a naïve ratio test to the higher orders given in [32], one concludes that the series (3.1) can be expected to converge for $\Delta^{-2} \lesssim 1$.

Now we proceed with the $\langle M\rangle = 1/3$ plateau of the *triangular lattice*, a case which has not been studied before. Recall that the triangular lattice has three sublattices and the lowest-energy state with $\langle M\rangle = 1/3$ is obtained by aligning all spins on two sublattices up and the ones on the third one down. The energy of this state at $h = 0$ is found to be

$$E_{1/3} = -JV\left(\frac{\Delta}{4} + \frac{1}{4\Delta} - \frac{1}{8\Delta^2} + \frac{19}{320\Delta^3}\right) + \mathcal{O}(\Delta^{-4}). \tag{3.3}$$

One possible excitation is obtained by flipping one further spin up. After a momentum decomposition, one can use non-degenerate perturbation theory to find the dispersion relation

$$\mathcal{E}_+(k_x, k_y) = J\left[3\Delta + \frac{\cos k_x + \cos k_y - \frac{3}{4} - 2(\cos k_x + \cos k_y)\cos(k_x + k_y) - \cos(k_x - k_y)}{\Delta}\right] + \mathcal{O}(\Delta^{-2}). \tag{3.4}$$

From its minimum one obtains the gap for $\delta S^z = 1$ excitations above the $\langle M\rangle = 1/3$ plateau:

$$\mathcal{E}_+(0,0) = \mathcal{E}_+\left(\frac{2\pi}{3}, \frac{2\pi}{3}\right) = 3J\Delta - \frac{15J}{4\Delta} + \frac{75J}{16\Delta^2} + \frac{783J}{320\Delta^3} + \mathcal{O}(\Delta^{-4}). \tag{3.5}$$

Now consider excitations with S^z smaller by 1 than in the $\langle M\rangle = 1/3$ plateau state. There are two possibilities for flipping a spin down with respect to the plateau state which are not related by translational symmetry. In order to minimize the energy one has to take the *difference* as a linear combination of these two possibilities. Then one finds, in a way similar to (3.4),

$$\begin{aligned}\mathcal{E}_-(k_x, k_y) = -J\Bigg[&\frac{1}{2}(\cos k_x + \cos k_y + \cos(k_x + k_y)) \\ &+ \frac{1}{\Delta}\left(\frac{7}{8} + \cos(k_x + k_y)(\cos k_x + \cos k_y - \cos k_x \cos k_y)\right. \\ &\left. - \frac{3}{4}(\cos(k_x + k_y) + \cos k_x + \cos k_y) + \cos k_x \cos k_y\right)\Bigg] + \mathcal{O}(\Delta^{-2}).\end{aligned} \tag{3.6}$$

Its minimum determines the gap for $\delta S^z = -1$ excitations above the $\langle M\rangle = 1/3$ plateau and is given by

$$\mathcal{E}_-(0,0) = -\frac{3J}{2} - \frac{5J}{8\Delta} + \frac{73J}{32\Delta^2} - \frac{42\,787\,J}{11\,520\,\Delta^3} + \mathcal{O}(\Delta^{-4}). \tag{3.7}$$

These series will be compared to results of a numerical diagonalization in the following sections.

We conclude this section by mentioning that the upper critical field h_{uc} at which the transition to a fully magnetized state takes place is straightforwardly computed exactly if it is

determined by a single spin flip. One finds

$$h_{uc} = \begin{cases} dJ(\Delta+1) & (d\text{-dimensional hypercubic lattice}) \\ 3J\left(\Delta+\dfrac{1}{2}\right) & (\text{triangular lattice}) \\ \dfrac{3}{2}J(\Delta+1) & (\text{hexagonal lattice}). \end{cases} \tag{3.8}$$

For later use we have actually given here the value of h_{uc} for the d-dimensional hypercubic lattice—the result for the square lattice is given by its $d = 2$ special case. Note that the overall numerical factor is proportional to the coordination number z of the lattice. Furthermore, for the bipartite lattices (hypercubic and hexagonal) one has $h_{uc} = (z/2)J(\Delta+1)$.

4. Numerical diagonalization for the square lattice

In this and the following sections we report results of a numerical study of the magnetization process for XXZ anisotropies around $\Delta = 1$. For a given Δ and magnetization we have numerically calculated the lowest eigenvalues of (1.1) with $h = 0$ in each momentum subspace applying Lanczos-type methods to a finite-size system. The magnetic field at which a transition between two states with different magnetization occurs is then calculated from the differences of the corresponding ground-state energies. This type of approach has been used in the literature for a long time (see e.g. [26, 27]) and below we therefore just present the consequences for the magnetization curves and skip the details of these standard (but still CPU-time-intensive) computations.

We choose to present our results in terms of 'magnetic phase diagrams'. They show the projection of the more conventional magnetization curves onto the axis of the magnetic field. The values of $\langle M\rangle$ are thus assigned to different regions of the plot. Since in this compact representation we save one axis, we can display the variation of the magnetization curves as a function of Δ in a single figure.

First we discuss the square lattice. This case has also been studied with finite-system diagonalizations at $\Delta = 1$ on a 4×4 lattice [16] as well as more recently on larger lattices [17]. At $\Delta = 1$ a second-order spin-wave investigation has also been performed [19]. For $\Delta > 1$ finite-system diagonalizations and quantum Monte Carlo simulations have been carried out in [18]. The system is therefore well understood and provides a good check of our method. Before presenting our results we recall from [18] that one finds a plateau with zero magnetization for $\Delta > 1$ whose boundary corresponds to a first-order phase transition, i.e. in the thermodynamic limit the magnetization jumps by a finite amount. This plateau disappears (its width tends to zero) as $\Delta \to 1$.

Figure 2 shows the magnetic phase diagram in the region with Δ close to one on a square lattice of size 4×6, i.e. with a volume of 24 spins. The thin full curves denote boundaries of the magnetization plateaux $\langle M\rangle = m/12$ ($m = 0, \ldots, 12$) which have to occur for this system size. For other system sizes other values for $\langle M\rangle$ will also be possible. Therefore, regions in figure 2 where these curves are regularly spaced can be expected to correspond to smooth transitions in the thermodynamic limit. Bearing this in mind, one can clearly see a plateau with magnetization $\langle M\rangle = 0$ in the right-hand half of figure 2. For a moderately accurate determination of its ending point we also use data on a 4×4 lattice. The linear approximation to the magnetization curve with a vanishing gap suggests as a criterion $16m_{4\times4}(\Delta_c) = 24m_{4\times6}(\Delta_c)$. This yields the estimate $\Delta_c \approx 0.87$.

It should also be noted that for $\Delta > 1.325$ the neighbour of $\langle M\rangle = 0$ has magnetization $1/6$, i.e. here it is favourable to flip two spins in the direction of the magnetic field rather than

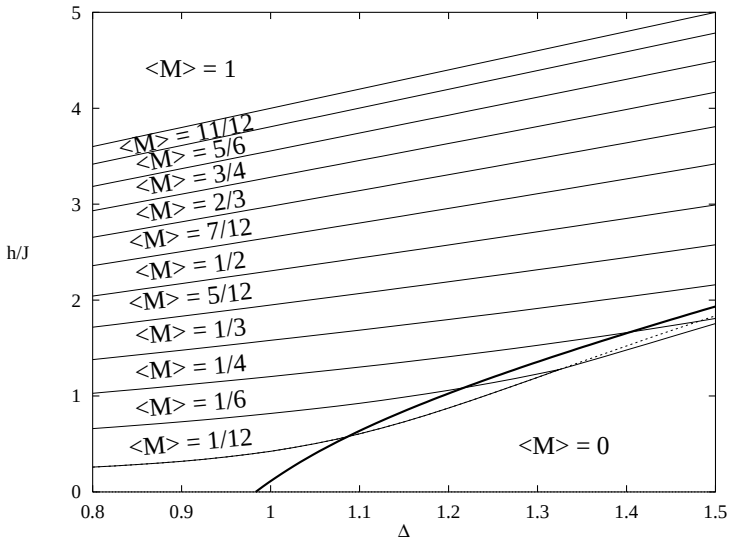

Figure 2. The magnetic phase diagram of the square-lattice XXZ antiferromagnet on a 4×6 lattice. The thin full curves denote boundaries of areas with the values of the magnetization indicated in the figure. The dashed curve is the spin gap (see the text). The bold full curve shows the extension to tenth order [32] of the series (3.1) for the gap.

one. This fact reflects the first-order nature of the transition. In this region $\Delta > 1.325$, the energy required for an excitation corresponding to a single flipped spin is shown by a dashed curve (otherwise the energy for such an excitation is equal to the boundary of the $\langle M\rangle = 0$ plateau: $h_{lc} = m$).

The extension to tenth order [32] of the series (3.1) is shown by the bold full curve in figure 2. Because the magnetic field required to close the spin gap is equal to its zero-field value, the series should be compared to the energy gap for a single flipped spin which is not always equal to the boundary of the $\langle M\rangle = 0$ plateau (in this case shown by the dashed curve). In the interval $1.1 < \Delta \leqslant 1.5$, this series slightly overshoots the finite-size data. In fact, the same can be observed in earlier presentations [18, 32] and therefore probably is due not to a finite-size effect but to missing higher-order terms in the series which could be quite important since we are looking at a region close to the limits of validity of this series ($\Delta \geqslant 1$ should be its region of convergence).

The fully magnetized state with $\langle M\rangle = 1$ gives rise to a further trivial plateau in figure 2. The finite-size data for its boundary agree with the analytical result (3.8), as they should.

Let us summarize our results for the square lattice. Using systems of size up 4×6 we are able to locate the end of the zero-magnetization plateau at $\Delta_c \approx 0.87$ which is a reasonable approximation to the presumably exact value $\Delta = 1$. Furthermore, the first-order nature of the transition is reflected in the fact that on a 4×6 lattice size it is favourable to flip two spins rather than one for $\Delta > 1.325$.

5. The triangular lattice, numerically

The triangular lattice was already studied some time ago by means of finite-system diagonalizations [12]. Now we can access larger system sizes and look more carefully at

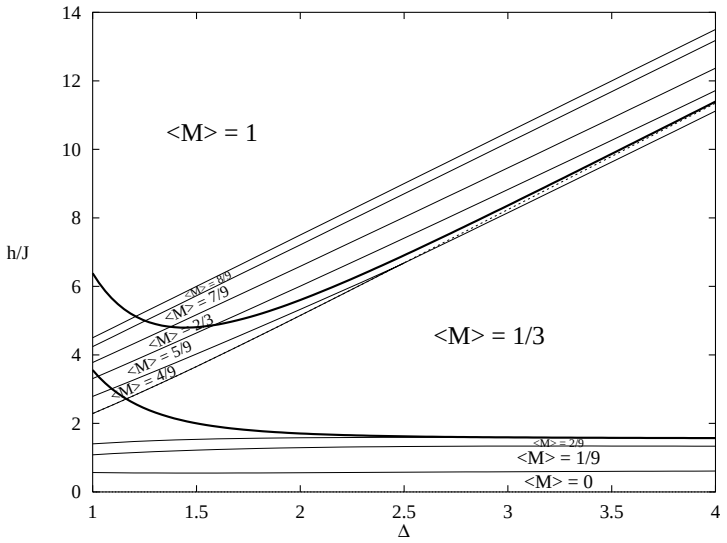

Figure 3. The magnetic phase diagram of the triangular-lattice XXZ antiferromagnet on a 3×6 lattice. The thin full curves denote boundaries of areas with the values of the magnetization indicated in the figure. The dashed curve is a single-spin excitation above the $\langle M \rangle = 1/3$ ground state (see the text). The bold full curves show the series (3.5) and (3.7).

the dependence on Δ†. To obtain an overview, we first look at the 3×6 lattice, even though precisely this lattice was already studied in [12] for $\Delta \in \{0.8, 1, 1.2, 2.5, 5\}$. Figure 3 shows our magnetic phase diagram for this case. The magnetization curves at $\Delta = 1$, 1.2 and 2.5 of [12] correspond to sections through figure 3 and are in all cases in excellent agreement with our results.

Here we observe precisely one non-trivial plateau with $\langle M \rangle = 1/3$. Note that for $\Delta \geqslant 2.4$ it becomes favourable to flip two spins rather than one at the upper boundary of this plateau. In this case, the energy of an excitation corresponding to a single spin flipped is shown by a dashed curve while the finite-size data for transitions between different ground states are shown by thin full curves. On the basis of our experience with the square lattice, we take this as an indication that the transition at the upper boundary of this plateau becomes first order for $\Delta \gtrsim 2$ while all other transitions are second order.

The series (3.5) and (3.7) for the upper $h_{c_2} = \mathcal{E}_+(0,0)$ and lower boundaries $h_{c_1} = -\mathcal{E}_-(0,0)$ of the $\langle M \rangle = 1/3$ plateau are shown by bold full curves. The former should be compared to the dashed curve, the latter to the appropriate thin full curve. The agreement is good for the right-hand half of figure 3. Since here we have fewer orders for the series than for the square lattice (figure 2), it is not surprising that the agreement in the region Δ close to one is less good. Again, the finite-size data for the location of the transition $\langle M \rangle \to 1$ agree exactly with (3.8).

Now we examine the region Δ close to one in more detail. First, we present the magnetization curve at $\Delta = 1$ in figure 4. The thin curves denote curves at three different system sizes. Here, we have used results of [14] to obtain the parts with $\langle M \rangle \leqslant 1/3$ of the magnetization curves with $V = 27$ and $V = 36$. Our results overlap with those of [14] just at the lower

† The current record for finite-system diagonalizations on this type of lattice seems to be held with a volume of 36 spins (see e.g. [14,34]). Since we want to vary the magnetization, wave vectors and Δ and still limit the computational effort, we content ourselves with smaller system sizes.

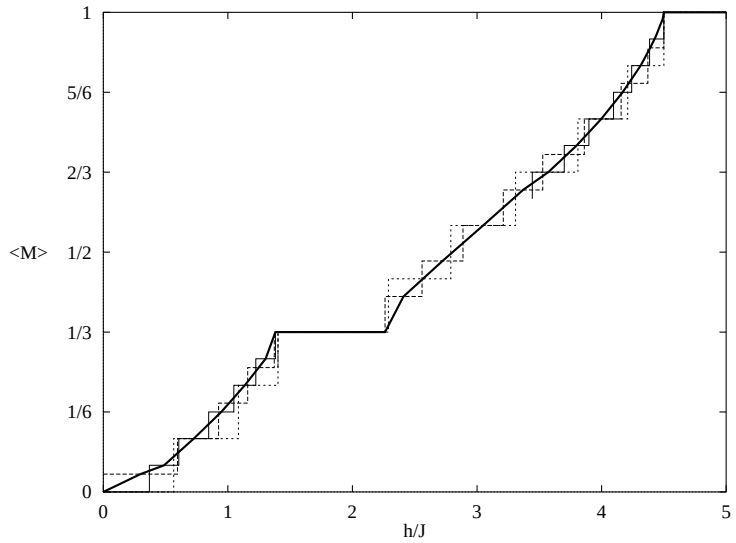

Figure 4. Magnetization curves of the spin-1/2 triangular-lattice Heisenberg antiferromagnet with $\Delta = 1$ on 3×6 (short dashes), $V = 27$ (long dashes) and $V = 36$ (thin full curve) lattices. The curves with volume $V = 27$ and $V = 36$ for $\langle M \rangle \leqslant 1/3$ are based on data of [14]. The bold full curve is an extrapolation to the thermodynamic limit (see the text).

boundary of the $\langle M \rangle = 1/3$ plateau at a volume $V = 27$. However, our geometry is different from that of [14]: in our computation the $V = 27$ lattice has a smallest spatial extent of just three sites while the configuration of [14] was designed to maximize the distance between boundaries. This leads to a difference of 2% between the results, which is reasonably small in view of the small linear size.

In figure 4 one can clearly see a plateau with $\langle M \rangle = 1/3$. The finite-size effects for its boundaries are small†. One observes that finite-size effects are also small for the mid-points of the steps in these curves, as is well known from one dimension [26, 27]. Drawing a curve through these points for the largest available system size (here we have used up to $V = 225 = 15 \times 15$ in the vicinity of the upper critical field h_{uc}), we therefore obtain the approximation to the thermodynamic limit shown by the bold full curve in figure 4.

Finally, in figure 5 we zoom in to the region Δ around one of figure 3, also using bigger system sizes‡ (figure 4 is a section at $\Delta = 1$ through figure 5). The main motivation for taking a closer look at this region comes from the observation in [12] that the $\langle M \rangle = 1/3$ plateau is present at $\Delta = 1$, but does not seem to exist at $\Delta = 0.8$. Inspecting figure 5 and paying attention to the finite-size effects (in particular the difference between the 3×6 and the 3×9 lattice), one concludes that this plateau presumably disappears somewhere in the region $\Delta \approx 0.85$.

We have also indicated the location of the $\langle M \rangle = 2/3$ plateau which is only realized for the 3×6 and the 6×6 lattice. However, the finite-size data provide no indication that it survives in the thermodynamic limit. So, it (and other possible plateaux) are likely to be absent in the thermodynamic limit, as is implied by the bold full curve in figure 4.

† The first-order spin-wave results for the boundaries of the $\langle M \rangle = 1/3$ plateau, $h_{c_1} \approx 1.248J$ and $h_{c_2} \approx 2.145J$ [13], are about $0.13J$ smaller than the finite-size diagonalization results.

‡ We have not computed all transition lines for the larger lattices sizes. We have omitted the ones for $\langle M \rangle < 1/3$ on the 3×9 lattice and those with $\langle M \rangle < 2/3$ on the 6×6 lattice.

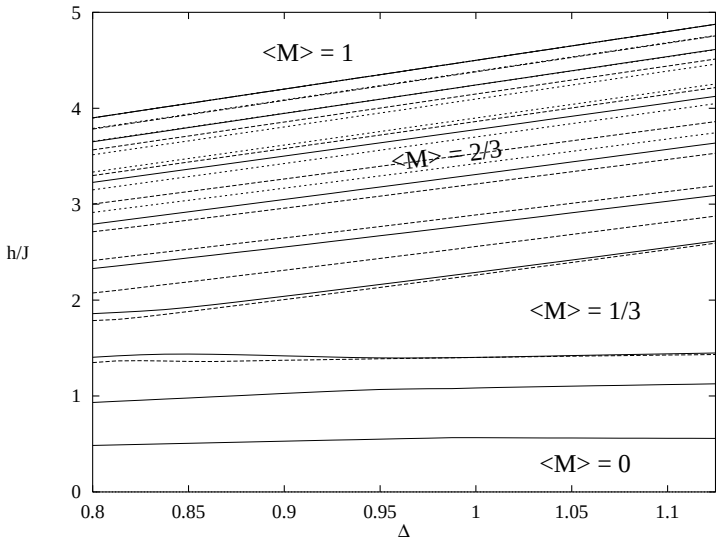

Figure 5. The magnetic phase diagram of the triangular-lattice XXZ antiferromagnet on a 3×6 (full curve), 3×9 (long-dashed curve) and 6×6 (short-dashed curve) lattice.

In figure 5 we have omitted the series (3.5) and (3.7), since in figure 3 one can already observe notable deviations in this region of Δ. Of course, the result (3.8) is still valid.

6. Numerical diagonalization for the hexagonal lattice

While the square lattice is self-dual, the dual of the triangular lattice is the hexagonal lattice. It is therefore interesting to also investigate the magnetization process on the hexagonal lattice. Figure 6 shows the results of diagonalizations on a 4×6 lattice. The region of small magnetization looks qualitatively very similar to that of the square lattice in figure 2. In particular, one can see an $\langle M \rangle = 0$ plateau (corresponding to the gap) for $\Delta \gtrsim 1$. Inferring from figure 6 that there is a first-order phase transition at the boundary of this plateau may be speculative, but this should also be expected on the grounds of universality, i.e. in the thermodynamic limit the transition at the boundary of the $\langle M \rangle = 0$ plateau for the hexagonal lattice should be in the same universality class as that of the square lattice. The location of the ending point of the $\langle M \rangle = 0$ plateau is compatible with $\Delta = 1$ (see also [33]) which would be the same for the square lattice. While in general one cannot use arguments based on universality to locate a critical point, here the point $\Delta = 1$ is distinguished by enhanced SU(2) symmetry and one may therefore expect the closing of the gap exactly at $\Delta = 1$.

The tenth-order version of [33] of the series (3.2) is shown by the bold full curve in figure 6 and should be compared with the dashed curve. The agreement is quite good close to the right-hand boundary of the figure and less good for smaller values of Δ. This is not surprising since the series for the hexagonal lattice [33] clearly converges less well than that for the square lattice [32].

As far as non-zero magnetizations are concerned, observe first that the transition to the fully magnetized state does indeed take place at the value of h_{uc} given by (3.8), thus giving a crosscheck on our computations. More important are the candidates for plateaux. In figure 6, the only plausible value for the appearance of a non-trivial plateau is at $\langle M \rangle = 1/2$.

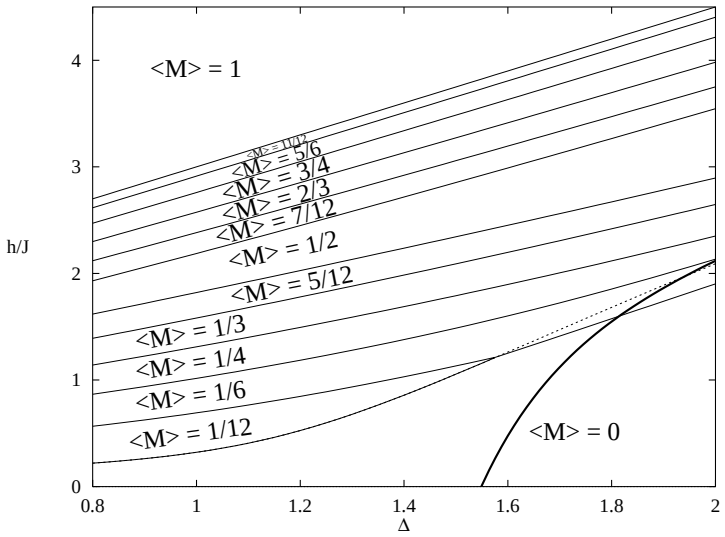

Figure 6. As figure 2, but for the hexagonal lattice. The bold full curve shows the extension to tenth order [33] of the series (3.2).

It should be noted that the geometry corresponding to figure 6 can be interpreted as a variant of the $N = 4$-leg spin ladder, and here plateaux are expected at $\langle M \rangle = 0$ and $\langle M \rangle = 1/2$ [4,5]. So, in order to see whether the wide step in figure 6 at $\langle M \rangle = 1/2$ is an intrinsic feature of the hexagonal lattice, one should look at other system sizes, and in particular larger strip widths. Since the large computational effort makes a systematic investigation of the dependence on Δ unfeasible, we have looked at the 6×6 lattice for a few selected values of Δ. The finite-size magnetization curves for $\Delta = 1$ in figure 7 are representative of the general case. In addition

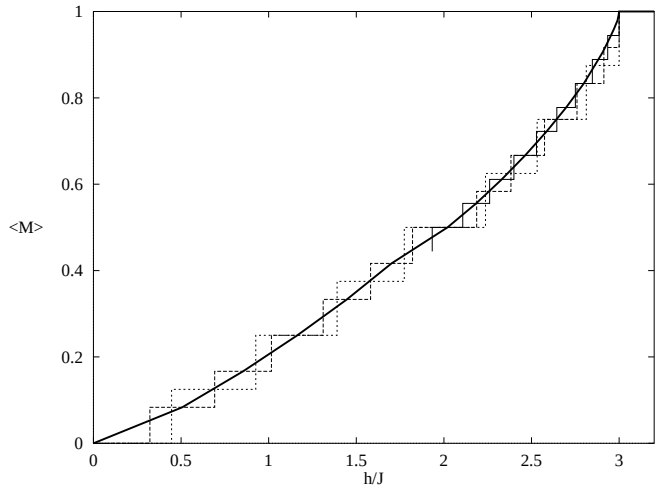

Figure 7. Magnetization curves of the hexagonal antiferromagnet with $\Delta = 1$. The finite-size data are for 6×6 (thin full curve), 4×6 (long dashes) and 4×4 (short dashes) lattices, respectively. As in figure 4, the bold full curve is an extrapolation to infinite volume.

to the data for the 4×6 lattice, we also show here magnetization curves for the 4×4 lattice and 6×6 lattice (close to saturation, some larger lattice sizes have also been considered, but are not explicitly shown).

With the data for the 6×6 lattice taken into account, there is no indication any longer of an $\langle M \rangle = 1/2$ plateau. The bold full curve therefore shows an extrapolated magnetization curve without plateaux, which as in figure 4 was obtained by connecting the mid-points of the steps for the largest available system sizes. This extrapolated curve shows that the 4×6 lattice is still subject to substantial finite-size effects which at $\langle M \rangle = 1/2$ combine to suggest a plateau.

Also at $\Delta = 2$ there is no evidence either for a plateau with $\langle M \rangle = 1/2$ on a 6×6 lattice (note that here the corresponding candidate in figure 6 on a 4×6 lattice is most pronounced). Thus, the final picture for the hexagonal lattice is the same as for the square lattice, i.e. the only plateau occurs for $\Delta > 1$ at $\langle M \rangle = 0$. The main qualitative difference between these two lattice types is in the finite-size corrections which are much more important for the hexagonal lattice.

7. The transition to saturation

Finally we look at the asymptotic behaviour of the magnetization as a function of the magnetic field close to saturation. One possibility is that it reaches the upper critical field h_{uc} following a power law. Then one would introduce a critical exponent μ via

$$1 - \langle M \rangle \sim \left(\frac{h_{uc} - h}{J} \right)^{\mu}. \tag{7.1}$$

A different possibility is a linear behaviour with a logarithmic correction:

$$1 - \langle M \rangle = a \left(\frac{h_{uc} - h}{J} \right) \ln \left(\frac{bJ}{h_{uc} - h} \right). \tag{7.2}$$

The latter has been argued in [19] to apply to the square-lattice antiferromagnet (see also [35, 36]).

To determine the functional form and estimate μ, we use the mid-point of the last step in the magnetization curve, as was done for the one-dimensional case e.g. in [37]. Since the corresponding magnetization satisfies $1 - \langle M \rangle = 2/V$, determination of the asymptotic behaviour of the magnetization curve is equivalent to determining the asymptotic finite-size behaviour of this last step. The particular choice of the mid-point of the step is not relevant for the determination of the exponent (or more generally, the functional form). Any other choice such as the last corner would simply yield a different prefactor. Values of such mid-points are given in table 1 for all three lattice types at the isotropic point $\Delta = 1$.

Fitting these data for the square lattice to the form (7.1), we find a value of μ in the region $\mu \approx 0.83$. However, the precise value increases if we use larger system sizes for the fit, as is expected to be the case in the presence of a logarithmic correction. Indeed, one obtains a better fit if one uses (7.2) instead. Using all data points for the square lattice in table 1 we find $a = 0.2505 \pm 0.0015$ and $b = 2.148 \pm 0.075$ where the errors indicate the $1\ \sigma$ confidence interval of the fit. So, the numerical data can be regarded as a confirmation of the functional form (7.2) predicted by first-order spin-wave theory [19], though it is not surprising that the values for the constants differ from the first-order spin-wave predictions [19] which, specialized to $S = 1/2$, are $a = 1/(2\pi)$, $b = \pi^2$. In no case do we reproduce the simple linear behaviour reported in [17]. The crucial difference is probably not that we employ exclusively system sizes which are larger than those used in [17], but that the analysis in this reference not only assumed the form (7.1), but also that $1/\mu$ is an integer.

Table 1. The mid-point of the last step before the upper critical field h_{uc} for two-dimensional antiferromagnets at $\Delta = 1$.

Square lattice		Triangular lattice		Hexagonal lattice	
V	$(h_{uc} - h)/J$	V	$(h_{uc} - h)/J$	V	$(h_{uc} - h)/J$
8×8	0.028767	6×6	0.057168	8×8	0.015650
10×10	0.016407	9×9	0.022087	10×10	0.0089914
12×12	0.010450	12×12	0.0094961	12×12	0.0057555
14×14	0.0071704	15×15	0.0054802	14×14	0.0039638
16×16	0.0051911	18×18	0.0035220	16×16	0.0028778
18×18	0.0039129	21×21	0.0024338	18×18	0.0021741
20×20	0.0030438	24×24	0.0017719	20×20	0.0016943
22×22	0.0024282	27×27	0.0013419	22×22	0.0013540
24×24	0.0019776	30×30	0.0010480	24×24	0.0011045
26×26	0.0016386	33×33	0.00083883	26×26	0.00091571

In the case of the triangular lattice, one should first discard the data for the volumes $V = 6 \times 6$ and $V = 9 \times 9$ in order to obtain a smooth curve. Then one again obtains the same behaviour as for the square lattice: the exponent μ obtained by the fit (7.1) has a very similar value and moves in the same direction with increasing V as for the square lattice. Furthermore, one obtains a better fit with (7.2) than with (7.1). Thus we conclude that the transition to saturation of the triangular lattice antiferromagnet also obeys (7.2), where the constants are now given by $a = 0.2991 \pm 0.0012$, $b = 1.249 \pm 0.030$.

For the hexagonal lattice we can access the same system sizes as for the square lattice. Thus, we can directly compare the values for the mid-points of the steps. One finds that those for the hexagonal lattice differ from the ones for the square lattice by a factor which rapidly approaches $\approx$0.56 with increasing system size. This means that the transitions to saturation of the square and hexagonal lattice should belong to the same universality class. Indeed, if we perform the same analysis as for the square lattice, we find the same behaviour for the hexagonal lattice. Just the constants for the fit (7.2) are different: now we have $a = 0.4338 \pm 0.0024$, $b = 1.527 \pm 0.052$.

In summary, we find support for the asymptotic behaviour (7.2) in all of the cases that we have considered. This universal behaviour can be understood in a way very similar to the Dzhaparidze–Nersesyan–Pokrovsky–Talapov (DN–PT) universal square root in one dimension [38, 39]. One starts from the single-particle excitations. At the transition field one starts to fill the lowest band of magnetic excitations. Generically, the dispersion around such a minimum is quadratic, e.g. $E \sim |\vec{k}|^2$. Then one needs to know how many states are available below this value of $|\vec{k}|$. In one dimension, where the detailed nature of the excitations does not matter, this number is proportional to k as long as one has an exclusion principle. Equivalently, for $d = 1$ the number of states available below a given energy E is proportional to $\sqrt{E}$. Since the magnetic field h acts as a chemical potential and the number of particles corresponds to the deviation of $\langle M \rangle$ from its critical value, this argument leads to the DN–PT universality class in one dimension.

For hard-core bosons in two dimensions (which is the situation that we consider here), interactions lead to a logarithmic correction to the naïve dimensional analysis [35, 36, 40] (see also chapter 6 of [41]) and thus to (7.2). Note however that this argument is independent of the details of the model under consideration. The crucial ingredients are just that the fundamental excitations are bosons with a quadratic dispersion around the minimum, subject to a repulsive interaction.

In three (and higher) dimensions we have Bose condensation. Therefore, the magnetization curve of a hypercubic antiferromagnet for $d \geqslant 3$ should have a simple linear approach to saturation [42]. Since this is the behaviour found for classical spins, the mean-field result for μ is in some sense exact for $d \geqslant 3$. The effect of Bose condensation which lowers μ substantially below the value $d/2$ can be observed clearly in numerical diagonalization of the isotropic (hyper)cubic antiferromagnet (compare table 2). In fact, if we fit the data in table 2 to the form (7.1), we find $\mu \approx 0.95$ for $d = 3$ and $\mu \approx 0.98$ for $d = 4$. Given the small linear extent of the systems considered, this is in reasonable agreement with the predicted value $\mu = 1$ without logarithmic corrections.

Table 2. The mid-point of the last step before the transition to saturation for the cubic and $d = 4$ hypercubic antiferromagnets at $\Delta = 1$.

$d = 3$		$d = 4$	
V	$(h_{uc} - h)/J$	V	$(h_{uc} - h)/J$
4^3	0.064954	4^4	0.022792
6^3	0.017227	6^4	0.0043387
8^3	0.0068532	8^4	0.0013508
10^3	0.0033871	10^4	0.00054895
12^3	0.0019148		
14^3	0.0011859		
16^3	0.00078466		
18^3	0.00054581		

Different values for μ can be obtained if the form of the dispersion close to the minimum is not quadratic. For example, for special values of parameters one could have $E \sim |\vec{k}|^4$ which for $d = 1$ leads to $\mu = 1/4$. The value $\mu = 1/4$ has been observed in the two-leg zigzag ladder [43] and the biquadratic spin-1 chain [44], each with a special value of the coupling constant. This is indeed explained by the aforementioned change in the single-particle dispersion (see [45] and [46], respectively).

8. Discussion and conclusions

In the present paper we have observed the following plateaux in magnetization curves. For the square and the hexagonal lattice, i.e. the two bipartite lattices, we find an $\langle M \rangle = 0$ plateau for $\Delta > 1$. The transition at the boundary of this plateau is likely to be always of first order. On the triangular lattice one finds a plateau with $\langle M \rangle = 1/3$ for $\Delta \gtrsim 0.85$. The transitions at its boundary appear to be second order for small enough anisotropies (at least for $\Delta \lesssim 2$).

Recently, plateaux with $\langle M \rangle = 1/2$ (and also $\langle M \rangle = 0$) have been observed on the triangular lattice with multi-spin interaction, in particular a four-spin interaction in addition to the two-spin interaction discussed in the present paper [47, 48]. At least the $\langle M \rangle = 1/2$ plateau survives even the classical limit [49]†. This is to be contrasted with the $\langle M \rangle = 1/3$ plateau in the triangular-lattice antiferromagnet which is absent in the classical limit and arises only in first-order spin-wave theory [13].

While all of the aforementioned plateaux with $\langle M \rangle \neq 0$ occur in frustrated systems, frustration is certainly not a necessary ingredient for the appearance of non-trivial plateaux. Consider for example a spin-1/2 N-layer square-lattice Heisenberg antiferromagnet (see [20]

† In addition, a plateau with $\langle M \rangle = 1/3$ can also be observed in the classical model for a suitable choice of parameters [49].

for a detailed discussion of the bilayer system in a magnetic field). In the limit where the in-plane coupling tends to zero, this system decouples into clusters of N spins. Simply by counting the possible states of these clusters, we conclude that plateaux exist with $\langle M \rangle = -1$, $-1 + 2/N, \ldots, 1 - 2/N, 1$ at least if the inter-plane coupling is much larger than the in-plane coupling [4, 5, 8]. However, frustration appears to favour the appearance of further plateaux. Therefore, a bilayer triangular lattice may be an interesting subject for further study.

The triangular and hexagonal lattices are dual to each other and thus share the same (local) point symmetry. However, we have seen that an antiferromagnet in a magnetic field behaves very differently on them. The point-symmetry group therefore does not appear to be of any relevance to the magnetization process. On the other hand, the square and hexagonal lattices share the property of being bipartite lattices and this in fact gives rise to very similar behaviour in the presence of a magnetic field.

In the classical or Ising limit, it is clear that the appearance of plateaux is related to the number of sublattices needed to describe the full magnetization process. It is therefore likely that some kind of translationally invariant unit cell will control the appearance of plateaux also in higher dimensions. The definition of such a unit cell in two dimensions is nevertheless far less obvious than in one dimension, and some ambiguity is also possible. To elucidate the situation further, it would be useful to study a wider range of models and lattice types. An important class of lattice types would be given by the eleven Archimedean tilings (see e.g. chapter 2 of [50]) among which we have considered the three monohedral ones. In particular, it would be interesting to investigate the magnetization process of the $S = 1/2$ Heisenberg model on the Kagomé lattice, where attention has so far been concentrated on the low-lying excitation spectrum (see [51] and references therein).

In a final part, we have numerically computed the asymptotic behaviour of the magnetization curve close to the transition to saturation. The fundamental excitations associated with this transition are hard-core bosons and one therefore finds a universal behaviour: the characteristic DN–PT square root in one dimension [38, 39], a linear behaviour with a logarithmic correction in two dimensions [19, 35, 36] and a simple linear behaviour in three and more dimensions [42]. This issue was studied for the transition to saturation because the diagonalization simplifies considerably in this limit. In particular, one can explicitly map the problem to a low-density gas of hard-core bosons. In one dimension, where the nature of the excitations is not really important, almost all second-order transitions at plateau boundaries are in the DN–PT universality class. So, presumably the universality class observed at the transition to saturation is also more general in higher dimensions. However, there is also room for different behaviour since now the natures of the fundamental excitations and the interactions are more important.

Acknowledgments

I am grateful to D C Cabra, M Kaulke, P Pujol, K D Schotte, M Troyer and M E Zhitomirsky for useful discussions. Some of the numerical computations were performed on computers of the Max-Planck-Institut für Mathematik, Bonn-Beuel.

References

[1] Manousakis E 1991 The spin-$\frac{1}{2}$ Heisenberg antiferromagnet on a square lattice and its applications to the cuprous oxides *Rev. Mod. Phys.* **63** 1–62

[2] Oshikawa M, Yamanaka M and Affleck I 1997 Magnetization plateaus in spin chains: 'Haldane gap' for half-integer spins *Phys. Rev. Lett.* **78** 1984–7

[3] Totsuka K 1997 Magnetization processes in bond-alternating quantum spin chains *Phys. Lett.* A **228** 103–10

[4] Cabra D C, Honecker A and Pujol P 1997 Magnetization curves of antiferromagnetic Heisenberg spin-$\frac{1}{2}$ ladders *Phys. Rev. Lett.* **79** 5126–9

[5] Cabra D C, Honecker A and Pujol P 1998 Magnetization plateaux in N-leg spin ladders *Phys. Rev.* B **58** 6241–57

[6] Totsuka K 1998 Novel massive ground states of spin chains in a magnetic field *Eur. Phys. J.* B **5** 705–17

[7] Cabra D C and Grynberg M D 1999 Ground state magnetization of polymerized spin chains *Phys. Rev.* B **59** 119–22

[8] Honecker A 1999 Strong-coupling approach to the magnetization process of polymerized quantum spin chains *Phys. Rev.* B **59** 6790–4

[9] Korshunov S E 1985 Antiferromagnetic XY model on a triangular lattice: ordered states in a magnetic field *JETP Lett.* **41** 641–3

[10] Dotsenko V S and Uimin G V 1985 Phase transitions in two-dimensional antiferromagnetic XY models in external fields *J. Phys. C: Solid State Phys.* **18** 5019–32

[11] Miyashita S 1986 Magnetic properties of Ising-like Heisenberg antiferromagnets on the triangular lattice *J. Phys. Soc. Japan* **55** 3605–17

[12] Nishimori H and Miyashita S 1986 Magnetization process in the spin-$1/2$ antiferromagnetic Ising-like Heisenberg model on the triangular lattice *J. Phys. Soc. Japan* **55** 4448–55

[13] Chubukov A V and Golosov D I 1991 Quantum theory of an antiferromagnet on a triangular lattice in a magnetic field *J. Phys.: Condens. Matter* **3** 69–82

[14] Bernu B, Lecheminant P, Lhuillier C and Pierre L 1994 Exact spectra, spin susceptibilities, and order parameter of the quantum Heisenberg antiferromagnet on the triangular lattice *Phys. Rev.* B **50** 10 048–62

[15] Suzuki N and Matsubara F 1997 Phase diagrams of the $S = \frac{1}{2}$ quantum antiferromagnetic XY model on the triangular lattice in magnetic fields *Phys. Rev.* B **55** 12 331–7

[16] Lozovik Y E and Notych O I 1993 Magnetization plateaux of frustrated antiferromagnet and analogy with FQHE *Solid State Commun.* **85** 873–7

[17] Yang M S and Mütter K-H 1997 The two dimensional antiferromagnetic Heisenberg model in the presence of an external field *Z. Phys.* B **104** 117–23

[18] Kohno M and Takahashi M 1997 Magnetization process of the spin-1/2 XXZ models on square and cubic lattices *Phys. Rev.* B **56** 3212–7

[19] Zhitomirsky M E and Nikuni T 1998 Magnetization curve of a square-lattice Heisenberg antiferromagnet *Phys. Rev.* B **57** 5013–16

[20] Troyer M and Sachdev S 1998 Universal critical temperature for Kosterlitz–Thouless transitions in bilayer quantum magnets *Phys. Rev. Lett.* **81** 5418–21

[21] Wu F Y, Wu X N and Blöte H W J 1989 Critical frontier of the antiferromagnetic Ising model in a magnetic field: the honeycomb lattice *Phys. Rev. Lett.* **62** 2773–6

[22] Inami T, Ajiro Y and Goto T 1996 Magnetization process of the triangular lattice antiferromagnets $RbFe(MoO_4)_2$ and $CsFe(SO_4)_2$ *J. Phys. Soc. Japan* **65** 2374–6

[23] Collins M F and Petrenko O A 1997 Triangular antiferromagnets *Can. J. Phys.* **75** 605–55

[24] Nojiri H, Tokunaga Y and Motokawa M 1988 Magnetic phase transition of helical $CsCuCl_3$ in high magnetic field *J. Physique Coll. Suppl.* **49** C8 1459–60

[25] Honecker A, Kaulke M and Schotte K D 1999 in preparation

[26] Bonner J C and Fisher M E 1964 Linear magnetic chains with anisotropic coupling *Phys. Rev.* **135** A640–58

[27] Parkinson J B and Bonner J C 1985 Spin chains in a field: crossover from quantum to classical behavior *Phys. Rev.* B **32** 4703–24

[28] Nightingale M P 1990 Transfer matrices, phase transitions, and critical phenomena: numerical methods and applications *Finite Size Scaling and Numerical Simulations of Statistical Physics* ed V Privman (Singapore: World Scientific) pp 287–351

[29] Bienenstock A and Lewis J 1967 Order–disorder of nonstoichiometric binary alloys and Ising antiferromagnets in magnetic fields *Phys. Rev.* **160** 393–403

[30] Schick M, Walker J S and Wortis M 1977 Phase diagram of the triangular Ising model: renormalization-group calculation with application to adsorbed monolayers *Phys. Rev.* B **16** 2205–19

[31] Honecker A 1996 A perturbative approach to spectrum and correlation functions of the chiral Potts model *J. Stat. Phys.* **82** 687–741

[32] Zheng Weihong, Oitmaa J and Hamer C J 1991 Square-lattice Heisenberg antiferromagnet at $T = 0$ *Phys. Rev.* B **43** 8321–30

[33] Oitmaa J, Hamer C J and Zheng Weihong 1992 Quantum magnets on the honeycomb and triangular lattices at $T = 0$ *Phys. Rev.* B **45** 9834–41

[34] Leung P W and Runge K J 1993 Spin-$\frac{1}{2}$ quantum antiferromagnets on the triangular lattice *Phys. Rev.* B **47**

5861–73
[35] Gluzman S 1993 Two-dimensional quantum antiferromagnet in a strong magnetic field *Z. Phys.* B **90** 313–18
[36] Sachdev S, Senthil T and Shankar R 1994 Finite-temperature properties of quantum antiferromagnets in a uniform magnetic field in one and two dimensions *Phys. Rev.* B **50** 258–72
[37] Hodgson R P and Parkinson J B 1985 Bethe *ansatz* for two-deviation states in quantum spin chains of arbitrary S with anisotropic Heisenberg exchange *J. Phys. C: Solid State Phys.* **18** 6385–95
[38] Dzhaparidze G I and Nersesyan A A 1978 Magnetic-field phase transition in a one-dimensional system of electrons with attraction *JETP Lett.* **27** 334–7
[39] Pokrovsky V L and Talapov A L 1979 Ground state, spectrum and phase diagram of two-dimensional incommensurate crystals *Phys. Rev. Lett.* **42** 65–7
[40] Popov V N 1972 On the theory of the superfluidity of two- and one-dimensional Bose system *Theor. Math. Phys.* **11** 565–73
[41] Popov V N 1983 *Functional Integrals in Quantum Field Theory and Statistical Physics* (Dordrecht: Reidel)
[42] Batyev E G and Braginskiĭ L S 1984 Antiferromagnet in a strong magnetic field: analogy with Bose gas *Sov. Phys.–JETP* **60** 781–6
[43] Schmidt M, Gerhardt C, Mütter K-H and Karbach M 1996 The frustrated antiferromagnetic Heisenberg model in the presence of a uniform field *J. Phys.: Condens. Matter* **8** 553–68
[44] Okunishi K, Hieida Y and Akutsu Y 1999 δ-function Bose gas picture of $S = 1$ antiferromagnetic quantum spin chains near critical fields *Phys. Rev.* B **59** 6806–12
[45] Cabra D C, Honecker A and Pujol P 1999 Magnetic properties of zigzag ladders *Preprint* cond-mat/9902112, BONN-TH-99-01, SISSA 10/99/EP, ETH-TH/99-01, ENSL-Th 02/99
[46] Golinelli O, Jolicoeur Th and Sørensen E S 1998 Incommensurability in the magnetic excitations of the bilinear–biquadratic spin-1 chain *Preprint* cond-mat/9812296, SPhT/98-120
[47] Misguich G, Bernu B, Lhuillier C and Waldtmann C 1998 Spin liquid in the multiple-spin exchange model on the triangular lattice: ^{3}He on graphite *Phys. Rev. Lett.* **81** 1098–101
[48] Momoi T, Sakamoto H and Kubo K 1999 Magnetization plateau in a two-dimensional multiple-spin exchange model *Phys. Rev.* B **59** 9491–9
[49] Kubo K and Momoi T 1997 Ground state of a spin system with two- and four-spin exchange interactions on the triangular lattice *Z. Phys.* B **103** 485–9
[50] Grünbaum B and Shephard G C 1987 *Tilings and Patterns* (New York: Freeman)
[51] Waldtmann Ch, Everts H-U, Bernu B, Sindzingre P, Lhuillier C, Lecheminant P and Pierre L 1998 First excitations of the spin 1/2 Heisenberg antiferromagnet on the Kagomé lattice *Eur. Phys. J.* B **2** 501–7